\WAS ANCIENT WINDBLOWN SAND LARGER THAN MODERN WINDBLOWN SAND ON MARS? GRAIN SIZE DISTRIBUTIONS IN THE STIMSON FORMATION, GALE CRATER, MARS, AND IMPLICATIONS FOR MARTIAN PALEOATMOSPHERE.

S. L. Preston[1], K. L. Siebach[1], and M. G. A. Lapôtre[2] [1]Department of Earth, Environmental and Planetary Sciences, Rice University, Houston, TX (slp7@rice.edu) [2]Department of Earth & Planetary Sciences, Stanford University, Stanford, CA

Introduction: Grain size distributions in eolian (windblown) sedimentary deposits encode information about the atmospheric conditions that enabled their transport and deposition as well as sediment supply. Sand in the Stimson sandstone, a unit of eolian sandstone in Gale crater, Mars, appears to be coarser than in the nearby Bagnold dunes, an active dune field [1, 2].

In this work, we measure grain size distributions in the Stimson sandstone and determine implications for the Martian paleoatmosphere. We also describe grain shape characteristics, such as roundness and sphericity, to constrain the sediment provenance of Stimson formation sandstones.

Geologic Context: Gale crater is a ~3.7 Ga impact crater with sedimentary strata exposed by wind forming a central mound called Mount Sharp that is the target of exploration for the Mars Science Laboratory rover *Curiosity* [3]. The current floor of Gale crater has a crater-count-based age of ~3 billion years, indicating that most of the crater filling and evacuating activity occurred during the Hesperian [4]. The Stimson formation is a relatively late sedimentary unit of dark-toned, cross-stratified sandstone that unconformably overlies the mound-forming unit called the Mt Sharp group [5]. It is interpreted as eolian due to its cross-stratification, stratigraphic context, and bimodal grain size (a detailed sedimentological analysis can be found in Banham et al. [4]). The Stimson outcrops at several locations along *Curiosity*'s traverse; this work focuses on the northernmost outcrops at the Emerson and Naukluft plateaus.

Grain Size Measurements: This work utilizes images from the Mars Science Laboratory *Curiosity* Mars Hand Lens Imager (MAHLI). MAHLI is a high-resolution imager mounted on the turret at the end of the rover's robotic arm, allowing close-up imagery of Alpha Particle X-Ray Spectrometer (APXS) targets. Most images used in this work have an image scale of ~31 µm/px, theoretically allowing resolution of grains as small as silt; in reality, dust often obscures fine grains. In this work, grains smaller than 4 pixels are omitted.

To measure grain size, we first sorted MAHLI images (n = 45) of APXS targets into 8 groups according to texture, then selected approximately two targets from each group, excluding soils and targets with diagenetic alteration. This approach was used to capture the range of textures within the Stimson sandstone while recognizing that the few high-resolution images taken by *Curiosity* may not be representative of the proportions of different textures in the overall unit. For the 12 targets representing 6 texture classes, we used the grid-by-number technique [1, 6] to select approximately 600 grains to measure, excluding grid points that did not have resolvable grains or that were obscured by dust.

Grains were outlined using the freehand selection tool in ImageJ [7], enabling automatic detection of the major and minor axes. Measurements were exported to CSV files for further analysis with GRADISTAT, a program that calculates grain size statistics [8]. Following these measurements, we found the weighted (according to texture group) average grain size distribution for APXS targets in the Stimson (Figure 1) had a mode of ~300 µm , a mean of 436.9 µm, a D_{50} of 331.8 µm, and a D_{90} of 857.4 µm. We are limited in observations of fine-grained and well-cemented targets; as such, this distribution is coarser than its true value. However, there is a significant fraction of coarser-than-expected grains across all targets. Previous work ([2]) found that active ripples in the Bagnold dunes have a mean grain size of 180 µm, a D_{50} of 141 µm, and a D_{90} of 329 µm.

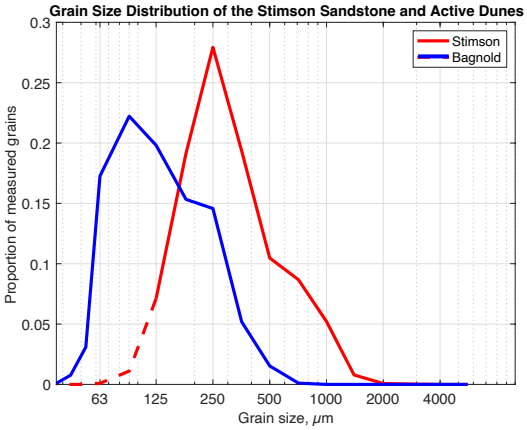

Figure 1. Grain size distribution of the Stimson (red) and Bagnold Dunes (blue, from [2]). Note that the Stimson is coarser overall than the Bagnold, and that the distributions are similar in width when plotted logarithmically. The distribution for the Stimson is poorly resolved below 125 µm.

Grain Properties. Across all non-diagenetic, non-altered Stimson targets, grains were generally dark-

toned and subrounded to rounded. Many coarse grains displayed pitting, consistent with eolian transport. There was no apparent correlation between grain color and grain size; light-toned grains, when present, were similar in size, roundedness, and pitting to the more common dark-toned grains, indicating that they were transported with the dark-toned grains. Targets in fracture halos were generally light-toned, well-rounded, pitted, and clast-supported with a light-toned matrix.

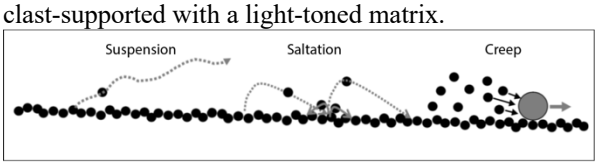

Figure 2. Schematic diagram of the primary modes of grain transport; modified from [6].

Eolian Sediment Transport: The Stimson is interpreted as a lithified dune field [5]; therefore, the sand was likely transported via saltation (Figure 2) rather than via creep or suspension [6]. Saltation initiates when the wind speed exceeds the threshold friction velocity, u^*_t, here estimated as

$$u_t^* = \sqrt{0.0123\left(\frac{\rho_s g d}{\rho_f} + \frac{\gamma}{\rho_f d}\right)}$$

(where ρ_s and ρ_f are the grain and atmospheric densities, respectively; g is the acceleration due to gravity; d is the grain diameter; and γ is a constant, typically valued at 3.0×10^{-4} kg s^{-2}) [6], and continues until wind speed drops below the impact threshold velocity u^*_i [9].

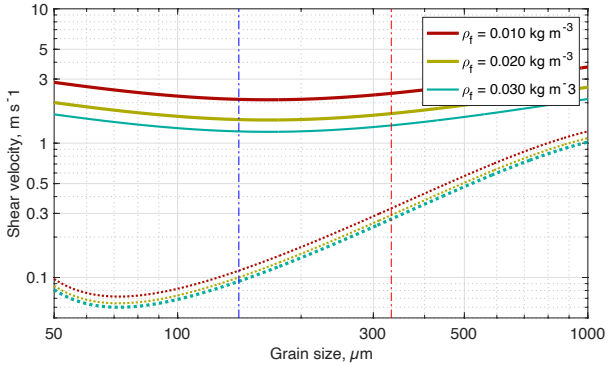

Figure 3. Threshold friction velocity (i.e., wind velocity required to initiate sand transport, u^*_t, solid lines) and impact threshold velocity (i.e., wind velocity required to sustain sand transport, u^*_i, dotted lines) for a variety of different atmospheric velocities; average atmospheric density measured by *Curiosity* is approximately 0.020 kg m^{-3} [11]. The D_{50} (dashed/dotted lines) for the Bagnold dunes (blue, [2]) and Stimson sandstone (red) are shown.

A denser atmosphere can initiate and continue transport of coarser grains than lower atmospheric densities for any given wind speed (Fig. 3); therefore, for a given supply of sand grains, it is more likely that a dense atmosphere would generate a coarser grain size distribution than a thin atmosphere. Whereas thin atmospheres could in principle transport a wider range of grain sizes via saltation due to transport hysteresis [10] (i.e., larger differences between the fluid and impact thresholds under thinner atmospheres), the distributions of modern and ancient sand sizes investigated herein appear to display similar widths (Fig. 1).

Implications for Stimson Provenance and Martian Paleoatmosphere: The grain size distribution of the Stimson sandstone appears to be coarser than that of the Bagnold dunes, including grains up to 1000 µm. Because the grains in the Stimson are generally well-rounded and pitted, their coarse size distribution can likely be attributed to their provenance and transport history rather than postdepositional alteration.

The optimal grain size for initiation of eolian transport (i.e., the grain size for which u^*_t is minimized) varies little with atmospheric density; assuming Martian gravity and a grain density of 2900 kg m^{-3}, the optimal grain size for transport is approximately 70–170 µm (Fig. 3). Even with the caveat that our measurements are biased towards coarser grains, the Stimson grains appear to be significantly coarser than the grains that were easiest to transport – regardless of atmospheric density. This suggests a coarse and nearby provenance for the Stimson, as well as a denser atmosphere to enable transport initiation for such coarse grains.

Acknowledgments: MAHLI image data for this project were collected from the PDS Geosciences Node Analyst's Notebook.

References: [1] Banham, S. G., et al. (2018) *Sedimentology, 65*, 993-1042. [2] Weitz, C. M., et al. (2018) *GRL, 45,* 9471-9478. .[3] Grotzinger, J. P., et al. (2015). *Science, 350.* [4] Grant, J. A., et al. (2014). *GRL, 41(4),* 1142-1149. [5] Watkins, J. A., et al. (2022) *JGR Planets, 127.* [6] Jerolmack, D. J., et al. (2006) *JGR Planets, 111.* [7] Rasband, W. S. (1997) *imagej.nih.gov/ij/.* [8] Blott, S. J. and Pye, K. (2001) *ESPL, 26(11),* 1237-1248. [9] Kok, J. F. (2010). *GRL 37(12).* [10] Goosmann, E. A., et al. (2018) *JGR Planets, 123,* 2506-2526. [11] Martínez, G. M., et al. (2017) *Space Science Reviews, 212(1)*, 295-338.